
A simple model for low frequency unsteadiness in compressible separated flows

S. Piponnier, P. Dupont, J.P. Dussauge, J.F. Debiève

Institut Universitaire des Systèmes Thermiques Industriels (IUSTI), Technopole de Château Gombert, 5 rue Enrico Fermi, 13453 MARSEILLE cedex 13

Abstract :

An aerodynamic model is proposed to explain the low frequency unsteadiness in Shock Wave / Boundary Layer Interactions, when the flow reattaches downstream. This model is based on mass entrainment in the mixing layer which develops at the edge of the recirculating zone, where the low frequency movements are linked to the successive contractions/dilatations of the recirculating bubble. This model has been applied for several experimental configurations, for Mach numbers from 0 to 5, and shows a good agreement with measurements.

1 Introduction

In many aeronautical applications, parameters of critical importance are imposed by unsteady conditions which can occur during flight, rather than by the steady ones. Although these events are rather rare or do not contribute much to the local averaged energy, they can correspond to locally high stresses, which can affect the whole behavior of the system. In supersonic flows, an important case is when the unsteadiness involves shock waves producing locally large pressure fluctuations. They may act as strong aerodynamic loads and are felt along the whole flow downstream of the shock wave. This is the case in shock induced separation, where low frequency unsteadiness is produced. The separated region and the shock wave system which develops upstream of the separation line oscillate at low frequency, at least two orders of magnitude lower than the energetic scales present in the upstream boundary layer. For decades, the interaction with an incident shock and the compression ramp have been the two most documented cases (see (1)). A recent review of the main properties of these flows can be found in (2). The origin of these low frequencies is not totally understood and several models have been suggested to explain their development. A major problem is to separate the low frequency shock motions, which appear when the flow is separating, from the motions related to the unsteady conditions of the upstream boundary layer. These last unsteadiness are typically based on upstream energetic scales and generate some corrugations of the shock wave, (3; 4; 5). The associated frequency scales differ by about two orders of magnitude from the low frequencies of the shock motions. Recently, significant improvement in the description of this low frequency unsteadiness has been obtained, both from experimental works (6; 7; 8; 9) and from numerical studies (10; 11; 12; 13). These results confirm that in the shock wave boundary layer interactions under consideration (compression ramp or impinging shock wave), low frequency movements of the separated region as well as motion of the shock wave which is formed upstream, are observed. Nevertheless, there are still some discrepancies in the analysis of the results.

Some authors found that the low frequency shock motions have to be related to the unsteady aspects of the upstream boundary layer (14). They invoke the large streamwise vortices formed in the upstream boundary layer, with a very large longitudinal lengthscale. Such large scale have been observed both experimentally (15) and numerically (16) and seem similar to the superstructures observed in subsonic turbulent boundary layer (17; 18).

Another approach is to suggest that the dynamics of the separated bubble has to be related to the shock movements. Several experimental work (19; 20; 6), and more recently numerical simulation, LES or DNS (21; 12; 13), observed this behaviour, but without being certain on the source of the unsteadiness. Do the shock movements influence the instantaneous position of the separated region through some upstream perturbations, or does the unsteadiness of the separated bubble impose the large motions of the shock ?

A compilation of different experiments, accessible through the literature, has been proposed by

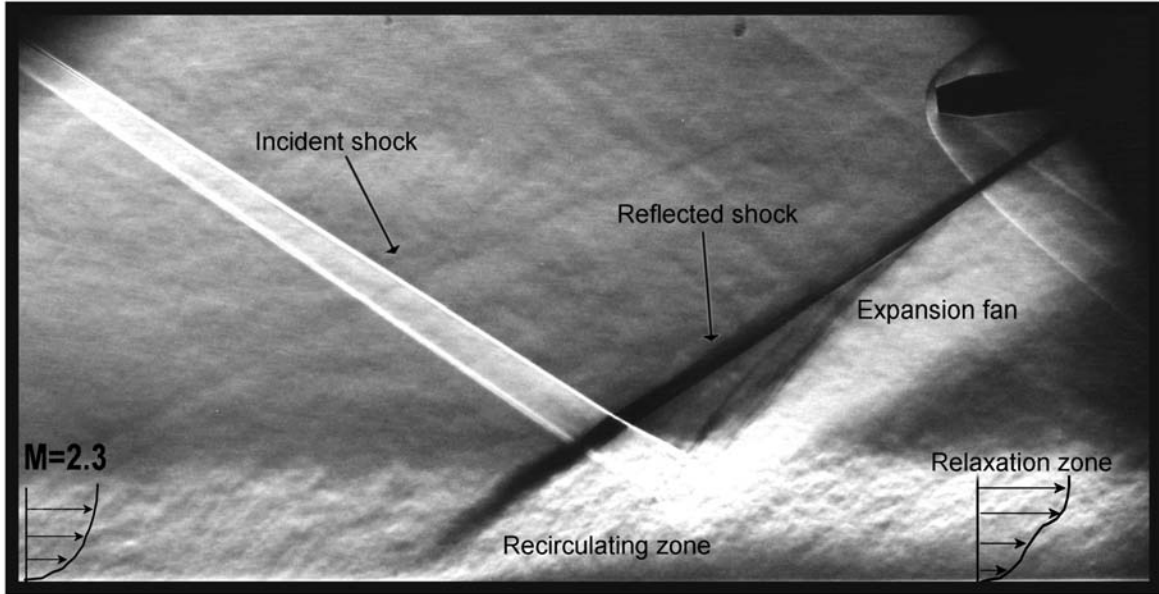


FIG. 1 – Spark Schlieren visualization of the interaction, flow deviation $\theta = 8^\circ$.

(22). The authors have calculated the dimensionless frequency of the unsteady shock wave (or Strouhal number S_L) in different cases, and add for reference the dimensionless frequency of a recirculating bubble in a subsonic detached flow (23). We observed that, for Mach number higher than 2, this Strouhal number is nearly constant ($S_L \simeq 0.03$), but is at least 4 times smaller than the subsonic case.

In this paper, we will propose to explain this fact through a simple analysis leading to define the main parametric dependence of this phenomenon, independently of the geometric conditions (compression corner, incident shock wave....) if the flow reattaches downstream. First a conditional analysis based on experimental results obtained in a Mach 2.3 oblique shock wave / turbulent boundary layer interaction as installed at IUSTI will be presented. Then the model will be explained, and finally, the parametric dependence will be checked vs. the data available in the literature

2 Experimental set-up

Measurements have been made using the supersonic wind tunnel of the IUSTI laboratory. The incoming boundary layer is turbulent fully developed. The test section is 120mm height by 170mm wide. The nominal Mach number is $M = 2.3$, the initial boundary layer thickness is $\delta_0 = 11\text{mm}$ and the Reynolds number, based on the momentum thickness, is $Re_{\delta_2} = 5.07 \times 10^5$. Measurements are obtained at a stagnation pressure of 0.5×10^5 Pa for a total temperature of 300°K . A shock generator made of a sharp-edged plate is fixed on the ceiling of the wind tunnel. It is placed in the free-stream and its leading edge is located in the potential flow. It spans the entire width of the test section and generates an oblique shock wave impinging on the floor boundary layer. Its angle with respect to the potential flow θ can be set continuously up to 10° .

The global organisation of the incident shock wave boundary layer interaction obtained by spark Schlieren visualisation is presented in figure 1. The flow deviation due to the incident shock is 8° , and the pressure gradient is strong enough for the layer to separate. In this case, the incident shock is reflected near the Mach line as an expansion wave, whereas the reflected shock originates upstream of the recirculating zone as described in (1). Velocity fields were obtained with PIV measurements, for an angle of the shock generator of $\theta = 9.5^\circ$. The PIV investigation was made using a Dantec Dynamics system. The light sheets were generated by a double pulse Nd :Yag laser New wave Solo II, which delivered 30 mJ per pulse, separated in time by $1\mu\text{s}$, and the particle images were recorded by Flowsense cameras (1600×1200). Measurements were made in vertical planes, along the longitudinal axis of the wind tunnel, in order to characterize the velocity fields along the interaction. In order to perform conditional

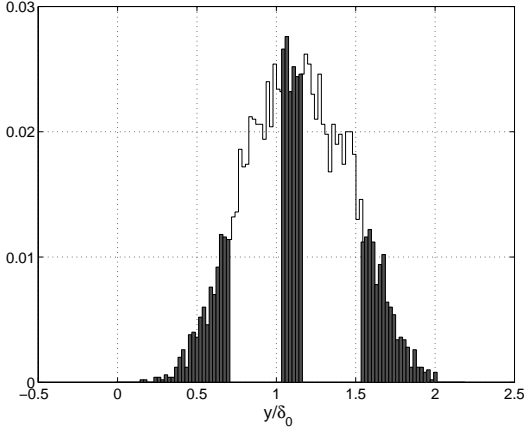


FIG. 2 – PDF of the instantaneous maximal elevation of the dividing stream line in the recirculating bubble.

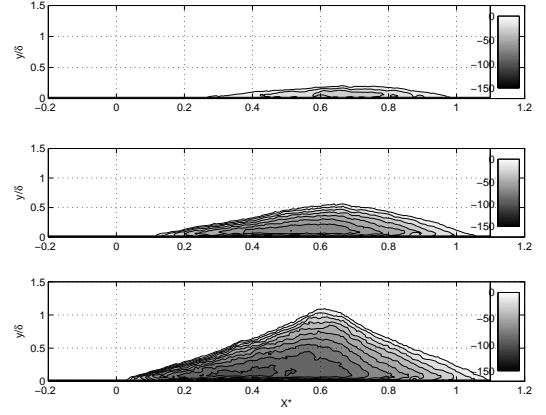


FIG. 3 – Conditional velocity fields; Only negative velocities, ranging between 0 and -150m/s are shown; ($\theta = 9.5^\circ$)

analysis of the velocity fields and to underline the unsteady breathing of the bubble and its connection with the unsteady shock motions, sets of 5000 digital images were acquired. the final PIV field of view is approximately $180 \times 20\text{mm}^2$ ($\simeq 16\delta_0 \times 2\delta_0$).

3 Conditionnal analysis of the sparated flow

Conditional analysis was applied to PIV velocity fields based on the instantaneous vertical extent of the recirculating region. The instantaneous dividing streamline was derived, and the unsteady recirculating bubble characteristics were sorted out, from the instantaneous elevation of the bubble defined as $y_{i,max} = \max(y_j(x))$, where the instantaneous dividing line $y_j(x)$ is defined as

$$\int_0^{y_j(x)} \rho u dy = 0 \quad (1)$$

The Probability Density Function of $y_{i,max}$ in the 9.5° case is shown in figure 3. We have selected three subsets of events :

- shallow bubbles : $y_{i,max}/\delta_0 < y_1$
- medium bubbles : $y_2 < y_{i,max}/\delta_0 < y_3$
- thick bubbles : $y_4 < y_{i,max}/\delta_0$.

The values y_i have been adjusted in such a way that each class represents about 10% of the data. The corresponding subsets are in grey tint on the histograms (see figure 3).

As we used 5000 fields to select the realizations, this gives roughly to about 500 samples for each subset. The corresponding conditional mean longitudinal velocity fields are reported in figure 3 for the 9.5° case. To highlight the recirculating region, grey scale is limited to the null or negative velocities. This underlines the highly variable behavior of the bubble.

We can see, at the light of this figure, that the recirculating bubble is clearly unsteady, with very large contractions and expansions. In the case of shallow bubbles, the bubble can be nearly suppressed. On the contrary, in the case of thick bubbles, the recirculating region is well spatially extended, with a maximum height of $y/\delta_0 \simeq 1.1$. The very high intensity of the reverse flow should be noted too : up to -150m/s , twice as large as the corresponding mean reverse flow velocity.

The behaviour of the recirculating bubble can be now considered : the bubble is very unsteady, with succession of contractions and expansions. This leads to events where the bubble is nearly suppressed, all of the fluid of the recirculating bubble has been absorbed by the main flow. And other events where there is a strong realimentation in fluid, with a maximum velocity of the backward flow which can be around 35% of the external upstream flow ! This intermittent behaviour can be supposed linked to the unsteady parts of the flow, as the unsteady separation shock and the incoming boundary layer.

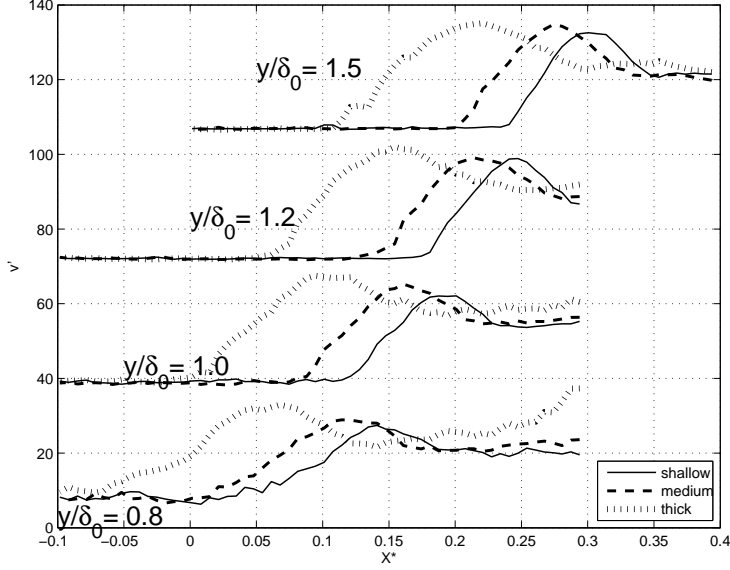


FIG. 4 – Conditional rms vertical fluctuations ($\theta = 9.5^\circ$).

4 Statistical links

For the same subsets of realizations, the conditionally averaged positions of the reflected shock have been estimated. We used the longitudinal evolution of the conditional normal velocity standard deviation ($\sqrt{v'^2}$) to localize the median position of the shock. In this analysis, the median position of the reflected shock is associated with an extremum for the rms velocity.

Results for 4 vertical positions are reported in figure 4. We see that the contractions of the bubble are related to downstream movements of the reflected shock whereas the dilatations are related to reverse flow of very high intensity and consequently to upstream movements of the reflected shock. The amplitude of the conditionally averaged positions of the reflected shock remain in the same proportion, if compared to L ($\simeq 0.1L$).

Finally, an asymmetry in the shock motions can be remarked. The shock displacement downstream from its mean position remains limited during the bubble contraction. In contrast, during the phase of large injection (strong dilatation of the recirculating bubble), the amplitude of the upstream shock motion is more than double.

With the same kind of analysis, it is possible to explore the possible link between the recirculating bubble and the incoming boundary layer. Nevertheless, no such statistical link could be identified, suggesting that the origin of the low frequency unsteadiness observed in this type of interaction can not be found in the incoming boundary layer.

5 Aerodynamic scheme

We propose here a simple analysis based on a global mass budget in the separated region. The aim is to build a scheme that can explain the breathing of the separated bubble occurring when a turbulent boundary layer separates under the effect of an adverse pressure gradient. We will not, at this point, discuss how this gradient is generated (deceleration, shock wave interaction, or other). Nor will we consider the presence of a shock upstream of the bubble. We will concentrate on the bubble itself. The separated zone is supposed to be of finite extent, with a spatial behavior as summarized in figure 5. In the first part of the bubble, that is from the separation line, eddies are formed in the mixing layer zone and grow as it moves downstream. In a quasi steady view, it may be assumed that fluid from the separated zone is entrained by the mixing layer. After some distance, these eddies are shed into the downstream flow, bringing with them their mass, momentum and vorticity outside the separated region. This generates, in the recirculating region, a default of mass that increases over time. Therefore, when the flow reattaches downstream, the mass amount inside the bubble decreases, and the steady separated

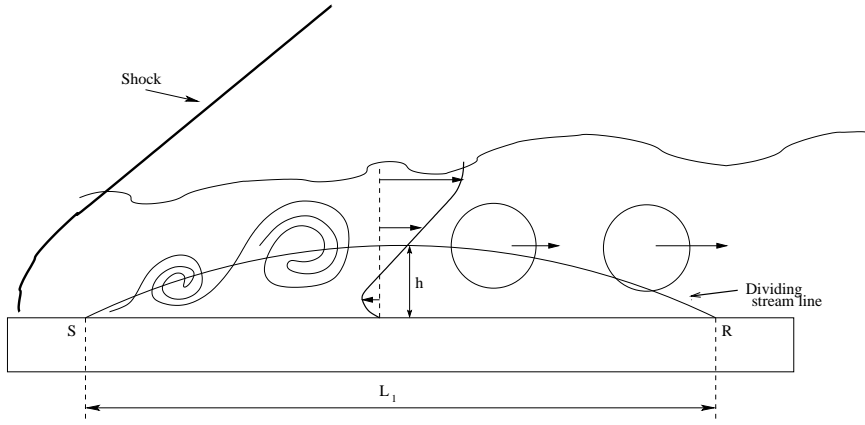


FIG. 5 – Sketch of the flow downstream the reflected shock.

situation cannot be maintained.

Consequently, there should be some flapping of the bubble which would let an air flux in the reverse direction occur with a time scale of T . The time scale required to entrain a significant amount of mass from the separated bubble obviously takes the form :

$$T = \text{mass in the reverse flow} / \text{rate of mass entrainment.}$$

After a time of the order of T , there is a significant deficit of mass in the separation and a necessity to insure a new amount of reverse flow from the downstream region, thus allowing the process to be repeated. We propose that the resulting large movements of the bubble are at the origin of the large amplitude shock motions. A similar scheme has already been proposed in both subsonic and supersonic cases (24; 12; 25) : here we propose to formulate it with simple hypotheses based on the dynamics of the equilibrium mixing layer. We will show that, in shock induced separated flows, high convective Mach numbers can easily be produced and that this mechanism becomes highly sensitive to compressibility effects. Therefore, the model will be developed in as general a form as possible, taking into account possible density effects, with characteristic Mach numbers ranging from 0 to supersonic values.

We can first evaluate the mass M_b of the initial recirculating bubble. If we approximate the bubble by a triangle of length L_1 and of height h (see figure 5), with an average density of ρ_m , then we have by unit span :

$$M_b = \frac{1}{2} \rho_m L_1 h \quad (2)$$

Here, h is the height of the bubble. We will therefore define h as the maximum elevation of the dividing line defined as the set of points $\{y_j(x)\}$ where $\int_0^{y_j(x)} \rho u dy = 0$. In subsonic separated flows ((24)) as well as in shock induced separated flows ((6)), the shedding of large structures that develop in the mixing layer occurs near of the middle of bubble, i.e. near $x = L_1/2$. Then, we can estimate the mass flux by unit span in the low velocity part of the mixing layer by :

$$M_{ej} = \int_{\delta_2(x=L_1/2)}^{y_0(x=L_1/2)} \rho u dy \quad (3)$$

where $\delta_2(x)$ is the edge of the mixing layer on the low velocity side and $y_0(x)$ the center line of the mixing layer.

The characteristic frequency could now be calculated, using some approximation on the mixing layers. The details of the calculation, not presented here, can be found in (26).

A new Strouhal number could be introduced, based on the mean height of the recirculating bubble h , and with the following expression :

$$S_h = \frac{fh}{u_1} = \Phi(M_c)g(r, s) \quad (4)$$

where $\Phi(M_c)$ is the normalized spreading rate and g is a function to be specified. Unfortunately, the quantity h is often not accessible in the literature, and the authors generally give only the

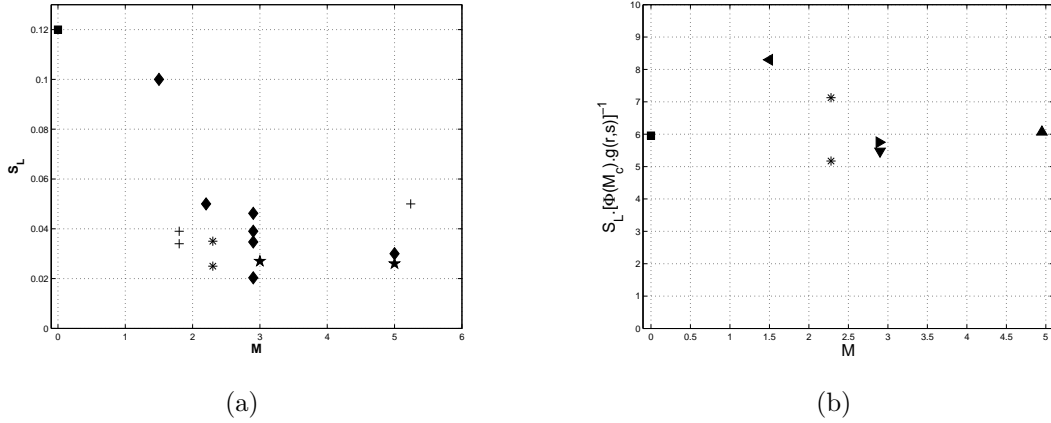


FIG. 6 – 6(a) : Strouhal number S_L in various configurations - 6(b) : Dimensionless frequency of the shock oscillation normalized as suggested by relation 5. (■) subsonic separation from (23), (*) IUSTI cases, (◄, ►, ▲, ▼) : compression ramps.

length of separation of the bubble (L_1) or the length of interaction (L). Therefore, we have to introduce another Strouhal number based on these length scales :

$$S_l = \frac{fl}{u_1} = \Phi(M_c)g(r, s) \frac{l}{h} \quad (5)$$

where l is the interaction length L , define as the length between the mean position of the reflected shock and the prolongation of the incident shock at the wall. If the separation length L_1 is retained (see figure 5), $\frac{L_1}{h}$ can be considered as the aspect ratio of the separated region. Unfortunately, this quantity is not well documented in the literature : in most of experimental works, only the length of interaction is available. In this case, the ratio $\frac{L}{h}$ will be considered as a crude approximation of the real aspect ratio of the bubble. Thus, for a given L/h , similar influences of the Mach number can be expected for S_L and for S_h .

The main result derived from relation 4 is the direct influence of the convective Mach number of the mixing layer through the function $\Phi(M_c)$. It is well known that this function is strongly Mach number dependent.

This model was compared to experimental results obtained on the experiments described in previous sections, and to others interactions in different flow configurations, with different Mach number, from experiments or numerical simulations. Results are presented on figure 6(b). The main Mach number effects seems to be reasonably well described. The mean value is around 6, as in the subsonic case (where the Strouhal number was $\simeq 0.12$), as for moderate and high Mach number ($2 < M < 5$), where the Strouhal number was around 0.03.

6 Conclusions

Low frequency unsteadiness in shock induced separation has been considered. A simple scheme based on the entrainment properties of the mixing layer which develops at the edge of the separation is proposed to explain their origin in the cases where the flow is reattaching downstream. The main parameters that influence the time scale are derived, and in particular, the dominant effect due to compressibility. This is related to large differences observed on low frequency flapping in subsonic and supersonic separated flows. The experimental results obtained in the IUSTI incident shock wave reflection are in very good agreement with the proposed model, while the action of the superstructures on the interaction does not give an appropriate value for the characteristic frequency in this experiment. Similarly, the low frequency shock unsteadiness observed in various shock induced separation, experimentally or from recent DNS and LES, are very well estimated from the model for a wide range of Mach numbers, independently of the particular geometry of the flow. The large decrease of the Strouhal number for upstream Mach number ranging from 0 to 2 and a saturation with a value of about 0.03 is well predicted : they are associated with the dramatic reduction of the compressible spreading rate of the mixing layer in this range of Mach numbers. Therefore, the main source of low frequency unsteadiness

in shock induced separated flows seems clearly to be the dynamics of the separated bubble.

The success in collapsing the data set of flows with relation 5 for a wide range of Mach numbers (from 0 to 5) and a wide range of Reynolds numbers (Re_δ from 3.7×10^4 to 144×10^4) suggests that the geometry of flow configurations does not have much influence on the results. Moreover, the proposed scaling does not use directly upstream frequency scales, so that the influence of the Reynolds number may appear only indirectly through the length scale h . This implies that, as supposed in the model, the initial development of the mixing layer defines the time constant of the bubble breathing and that the downstream history of the flow, in the vicinity of the reattachment line, is not a key factor for the unsteadiness of the interaction. A final result can be derived from the compilation reported in figure 6(b). As already mentioned, the quantity $S_L \times \{g(r, s)\Phi(M_c)\}^{-1}$ can be related to the aspect ratio of the interaction zone : L/h (see eq. 5). Therefore it seems that these different interactions have very similar aspect ratios, around 6.

However, the present model, which explicitly takes in account compressibility effects inside the separated bubble, gives a consistent and efficient way to represent shock unsteadiness in two dimensional shock induced separation for a wide range of Mach numbers.

Acknowledgments

Part of this work was carried out with support from the Research Pole CNES/ONERA *Aérodynamique des Tuyères et Arrière-Corps* (ATAC) and a grant of the European STREP UFAST (contract n° AST4-CT-2005-012226). Their support is gratefully acknowledged.

Références

- [1] Delery J. and Marvin J. Shock wave - boundary layer interactions. Technical report, 1986.
- [2] Dolling D. Fifty years of shock-wave/boundary-layer interaction research : what next. AIAA Journal, Vol. 39, n°8, 1517–1531, aug 2001.
- [3] Debiève J. and Lacharme J. A shock wave/free turbulence interaction. In IUTAM Symposium on Turbulent Shear-Layer/Shock-Wave Interaction, Palaiseau, France, september 9-12 1985.
- [4] Wu M. and Miles R. B. Megahertz visualization of compression-corner shock structures. AIAA Journal, Vol. 39, No. 8, 1542–1546, August 2001.
- [5] Garnier E. and Sagaut P. Large eddy simulation of shock/ boundary layer interaction. AIAA Journal, Vol. 40, n°10, 1935–1944, oct 2002.
- [6] Dupont P., Haddad C., and Debiève J. Space and time organization in a shock induced boundary layer. J. Fluid Mech., Vol. 559, 255–277, 2006.
- [7] Ganapathisubramani B., Clemens N., and Dolling D. Effects of upstream coherent structures on low-frequency motion of shock-induced turbulent separation. In 45th AIAA Aerospace Sciences Meeting and Exhibit, Reno, Nevada, 8-11 January, 2007.
- [8] Dupont P., Piponnier S., Sidorenko A., and Debiève J. Investigation of an oblique shock reflection with separation by piv measurements. AIAA Journal, Vol. 46 no. 6, june 2008.
- [9] Souverein L., Oudheusden B., Scarano F., and Dupont P. Unsteadiness characterisation in a shock wave turbulent boundary layer interaction through dual- PIV. In 38th Fluid Dynamics Conference and Exhibit 23 - 26 June 2008, Seattle, Washington, 2008.
- [10] WU M. and Martin M. P. Direct numerical simulation of supersonic turbulent boundary layer over a compression ramp. AIAA Journal, Vol. 45, N°4, 879–889, apr 2007.
- [11] de Martel E., Garnier E., and Sagaut P. Large eddy simulation of impinging shock wave / turbulent boundary layer interaction at $M=2.3$. In IUTAM Symposium on Unsteady Separated Flows and their Control, Corfu, Greece, june 18-22 2007.

-
- [12] Wu M. and Martin M. P. Analysis of shock motion in shockwave and turbulent boundary layer interaction using direct numerical simulation data. *J. Fluid Mech.*, Vol. 594, 71–83, jan 2008.
- [13] Touber E. and Sandham N. Oblique shock impinging on a turbulent boundary layer : low-frequency mechanisms. In 38th AIAA Fluid Dynamics Conference, 23-26 June, Seattle, 2008.
- [14] Beresh S., Clemens N., and D.S.Dolling . Relationship between upstream turbulent boundary layer velocity fluctuations and separation shock unsteadiness. *AIAA Journal*, Vol. 40, n°12, 2412–2422, dec 2002.
- [15] Ganapathisubramani B., Clemens N., and Dolling D. Large-scale motions in a supersonic turbulent boundary layer. *Journal of Fluid Mechanics*, 556, 271–282, 2006.
- [16] Ringuette M., Wu M., and Martin M. P. Coherent structures in direct numerical simulation of turbulent boundary layers at Mach 3. *J. Fluid Mech.*, 594, 59–69, 2008.
- [17] Kim K. C. and Adrian R. J. Very large-scale motion in the outer layer. *Phys. Fluids*, 11, 417–422, 1999.
- [18] Adrian R. J., Meinhart C. D., and Tomkins C. D. Vortex organization in the outer region of the turbulent boundary layer. *J. Fluid Mech.*, 422, 1–53, 2000.
- [19] Thomas F., Putman C., and CHU H. On the mechanism of unsteady shock oscillation in shock wave/turbulent boundary layer interaction. *Experiments in Fluids*, Vol. 18, 69–81, 1994.
- [20] Erenkil M. and Dolling D. Unsteady wave structure near separation in a Mach 5 compression ramp interaction. *AIAA Journal*, Vol. 29, N°5, 728–735, may 1991.
- [21] Pirozzoli S. and Grasso F. Direct numerical simulation of impinging shock wave / turbulent boundary layer interaction at $M=2.25$. *Physics of Fluid*, 18, 2006.
- [22] Dussauge J., Dupont P., and Debiève J. Unsteadiness in shock wave boundary layer interactions with separation. *Aerospace Science and Technology*, Vol. 10, 85–91, 2006.
- [23] M.Kiya and Sasaki K. Structure of a turbulent separation bubble. *J. Fluid Mech.*, Vol. 137, 83–113, 1983.
- [24] Cherry N., Hillier R., and Latour M. Unsteady measurements in a separated and reattaching flow. *J. Fluid Mech.*, Vol. 144, 13–46, 1984.
- [25] Dandois J., Garnier E., and Sagaut P. Numerical simulation of active separation control by synthetic jet. *J. Fluid. Mech.*, 574, 25–58, 2007.
- [26] Piponniau S., Dussauge J., Debieve J., and Dupont P. A simple model for low frequency unsteadiness in shock induced separation. *J. Fluid Mech.*, (629), 87–108, June 2009.